

Mechanistic Comparison of Thermal and Photochemical Intramolecular Electron-Transfer Reactions: Differentiation on the Basis of Remarkably Different Pressure Dependencies

Pilar Guardado^{1a} and Rudi van Eldik^{*1b}

Received December 18, 1989

The kinetics of the electron-transfer reaction between $\text{Co}(\text{NH}_3)_4(\text{pzc})^{2+}$, $\text{Co}(\text{en})_2(\text{pzc})^{2+}$, and $\text{Co}(\text{NH}_3)_5\text{pz}^{3+}$ (where pz = pyrazine and pzc = pyrazinecarboxylate) and $\text{Fe}(\text{CN})_5\text{H}_2\text{O}^{3-}$ was studied as a function of concentration, temperature, pressure, and light intensity of the analyzing beam. These reactions exhibit two kinetic steps: formation of pz- and pzc-bridged complexes followed by intramolecular electron transfer. The first step is characterized by large positive volumes of activation (between +23 and +28 $\text{cm}^3 \text{mol}^{-1}$), which are interpreted in terms of a dissociative mechanism involving the breakage of the $\text{Fe}^{\text{II}}-\text{H}_2\text{O}$ bond. The intramolecular electron-transfer reaction also exhibits large positive volumes of activation (between +27 and +37 $\text{cm}^3 \text{mol}^{-1}$), which disappear almost completely for the photoinduced electron-transfer reaction. These results are interpreted and discussed in reference to related data reported in the literature.

Introduction

The application of high-pressure kinetic techniques in the elucidation of inorganic and organometallic reaction mechanisms has gained significant support over the past decade.^{2,3} By far the majority of the available activation volume data are for thermally induced ligand substitution reactions, which has resulted in a systematic differentiation of the underlying mechanisms.^{4–8} In comparison, the data available for photoinduced substitution reactions^{9,10} were interpreted along similar lines and have lately been demonstrated to be a powerful mechanistic indicator.¹¹ Although some activation volume data are available for thermal electron-transfer reactions,^{3,12} almost no data is available for photoinduced electron-transfer reactions,^{3,10} thus making a comparison of the mechanisms based on such data rather impossible.

In search for such a possible correlation, we have selected a few intramolecular electron-transfer systems that exhibit very large volumes of activation (as large as +38 $\text{cm}^3 \text{mol}^{-1}$) for the thermal reaction, and in addition exhibit photoinduced electron-transfer reactions.^{13–15} In this respect, Sasaki et al.¹³ reported a value of +38 $\text{cm}^3 \text{mol}^{-1}$ for the thermal intramolecular electron-transfer reaction in $(\text{NH}_3)_5\text{Co}^{\text{III}}(\mu\text{-pz})\text{Fe}^{\text{II}}(\text{CN})_5$, where pz = pyrazine, whereas Bin Ali et al.¹⁴ reported +24 $\text{cm}^3 \text{mol}^{-1}$ for the corresponding bis(ethylenediamine) pyrazinecarboxylate-bridged complex. In addition, these and other closely related complexes exhibit photoinduced electron-transfer reactions.¹⁵ We have found a remarkable difference in the pressure sensitivity of the thermal and photochemical electron-transfer processes that enable us to comment in detail on the underlying reaction mechanisms.

Experimental Section

Materials. The complexes $[\text{Co}(\text{en})_2(\text{pzc})](\text{ClO}_4)_2$, $[\text{Co}(\text{NH}_3)_4(\text{pzc})](\text{ClO}_4)_2 \cdot 2\text{H}_2\text{O}$ and $[\text{Co}(\text{NH}_3)_5\text{pz}](\text{ClO}_4)_3$, where pz = pyrazine and pzc = pyrazinecarboxylate, were prepared according to the methods

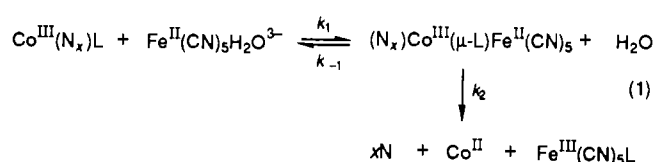
described in the literature.^{15,16} Sodium nitroprusside was treated with concentrated aqueous NH_3 to yield $\text{Na}_3[\text{Fe}(\text{CN})_5\text{NH}_3]$,^{17,18} which on dissolution in water immediately gives the $\text{Fe}(\text{CN})_5\text{H}_2\text{O}^{3-}$ species. Chemical analyses and UV-vis spectral data of all isolated complexes were in good agreement with the theoretically expected values and those reported in the literature, respectively. All chemicals used were analytical reagent grade. Deionized water was used as solvent throughout this study. The ionic strength of the medium was adjusted to 0.1 M with NaClO_4 . Special care was taken to perform kinetic measurements on fresh solutions of $\text{Fe}(\text{CN})_5\text{H}_2\text{O}^{3-}$ because this species tends to degrade slowly.¹⁹ All test solutions were deoxygenated immediately before use.

Instrumentation. UV-vis absorption spectra were recorded on a Shimadzu UV 250 spectrophotometer using a thermostated (+0.1 °C) cell compartment. Kinetic measurements at ambient pressure were performed with the aid of an Aminco stopped-flow unit, and at pressures up to 100 MPa on a homemade high-pressure stopped-flow system.²⁰ A xenon light source was used in both these systems, which proved to be an excellent source to induce the photochemical redox reactions. The light intensity was controlled through the slit width of the monochromator. Both stopped-flow units were thermostated to within ± 1 °C. Slower reactions were either studied in the thermostated cell compartment of the spectrophotometer or in a high-pressure cell linked up to a Zeiss PMQ II spectrophotometer system operating in the double-beam mode.²¹

Kinetic Measurements. All investigated reactions were studied under first-order or pseudo-first-order conditions. The stopped-flow data were treated on an online data acquisition system.²² All first-order plots were linear for at least 2–3 half-lives of the reaction.

Results and Discussion

The mechanistic behavior of intramolecular electron-transfer reactions can in general be described in terms of the mechanism outlined in (1), which consists of a rapid complex formation

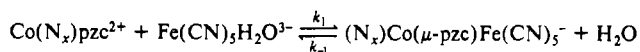


L = pyrazinecarboxylate; $\text{N}_x = (\text{en})_2$
(en = ethylenediamine), $(\text{NH}_3)_4$

L = pyrazine; $\text{N}_x = (\text{NH}_3)_5$

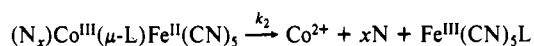
- (1) (a) On leave from the Department of Physical Chemistry, University of Sevilla, 41012 Sevilla, Spain. (b) University of Witten/Herdecke.
- (2) van Eldik, R., Ed.; *Inorganic High Pressure Chemistry: Kinetics and Mechanisms*; Elsevier: Amsterdam, 1986.
- (3) van Eldik, R.; Asano, T.; le Noble, W. J. *Chem. Rev.* **1989**, *89*, 549.
- (4) Merbach, A. E. In ref 2, Chapter 2.
- (5) van Eldik, R. In ref 2, Chapter 3.
- (6) Kotowski, M.; van Eldik, R. In ref 2, Chapter 4.
- (7) Curtis, N. J.; Lawrance, G. A.; van Eldik, R. *Inorg. Chem.* **1989**, *28*, 329.
- (8) Awad, H. H.; Dobson, C. B.; Dobson, G. R.; Leipoldt, J. G.; Schneider, K.; van Eldik, R.; Wood, H. E. *Inorg. Chem.* **1989**, *28*, 1654.
- (9) DiBenedetto, J.; Ford, P. C. *Coord. Chem. Rev.* **1985**, *64*, 361.
- (10) Ford, P. C. In ref 2, Chapter 6.
- (11) Wieland, S.; van Eldik, R. *J. Chem. Soc., Chem. Commun.* **1989**, 367.
- (12) Swaddle, T. W. In ref 2, Chapter 5.
- (13) Sasaki, Y.; Ninomiya, T.; Nagasawa, A.; Endo, K.; Saito, K. *Inorg. Chem.* **1987**, *26*, 2164.
- (14) Bin Ali, R.; Blandamer, M. J.; Burgess, J.; Guardado, P.; Sanchez, F. *Inorg. Chim. Acta* **1987**, *131*, 59.
- (15) Malin, J. M.; Ryan, D. A.; O'Halloran, T. V. *J. Am. Chem. Soc.* **1978**, *100*, 2097.

- (16) Toma, H. E. *J. Inorg. Nucl. Chem.* **1975**, *37*, 785.
- (17) Manchot, W.; Merry, E.; Woring, P. *Chem. Ber.* **1912**, *45*, 2869.
- (18) Ernhofer, R.; Kovacs, D.; Subak, E.; Shepherd, R. E. *J. Chem. Educ.* **1978**, *55*, 610.
- (19) Toma, H. E.; Malin, J. M. *Inorg. Chem.* **1973**, *12*, 1039.
- (20) van Eldik, R.; Palmer, D. A.; Schmidt, R.; Kelm, K. *Inorg. Chim. Acta* **1981**, *50*, 131.
- (21) Fleischmann, F. K.; Conze, E. G.; Stranks, D. R.; Kelm, H. *Rev. Sci. Instrum.* **1974**, *45*, 1427.
- (22) Kraft, J.; Wieland, S.; Kraft, U.; van Eldik, R. *GIT Fachz. Lab.* **1987**, *31*, 560.

Table I. k_{obs} as a Function of [Co(III)], Temperature, and Pressure for the Formation of the Bridge Complex According to the Reaction^a

N_x	temp, °C	pressure, MPa	$10^4[\text{Co(III)}], \text{M}$	$k_{\text{obs}}^b, \text{s}^{-1}$	$10^{-3}k_1, \text{M}^{-1} \text{s}^{-1}$	k_{-1}, s^{-1}					
$(\text{NH}_3)_4$	19.9	0.1	2	0.92 ± 0.02	2.03 ± 0.04	0.54 ± 0.03					
			4	1.36 ± 0.02							
			5	1.59 ± 0.01							
			8	2.16 ± 0.02							
			10	2.56 ± 0.03							
	25.0			4	2.12 ± 0.03	3.49 ± 0.05	0.71 ± 0.04				
				6	2.76 ± 0.03						
				8	3.49 ± 0.14						
				10	4.21 ± 0.05						
				30	9.22 ± 0.27						
	30.0			4	3.29 ± 0.13	6.00 ± 0.12	0.84 ± 0.09				
				5	3.76 ± 0.12						
				6	4.43 ± 0.16						
				8	5.68 ± 0.09						
				10	6.82 ± 0.46						
	35.0			2	2.40 ± 0.03	10.4 ± 0.9	0.62 ± 0.50				
				4	5.12 ± 0.21						
				6	7.14 ± 0.05						
				8	8.69 ± 0.22						
				10	8.69 ± 0.22						
	24.3	5		2	0.94 ± 0.02	2.9 ± 0.3	0.22 ± 0.18				
				4	1.15 ± 0.03						
				6	1.96 ± 0.10						
				8	2.67 ± 0.08						
				10	3.06 ± 0.04						
		25			2	0.65 ± 0.02	2.6 ± 0.3	-0.23 ± 0.18			
					4	0.92 ± 0.04					
					6	1.38 ± 0.06					
					8	2.22 ± 0.06					
					10	2.59 ± 0.06					
50				2	0.49 ± 0.01	1.8 ± 0.2	0.01 ± 0.10				
				4	0.61 ± 0.04						
				6	1.12 ± 0.06						
				8	1.44 ± 0.03						
				10	1.91 ± 0.06						
75			2	0.36 ± 0.01	1.5 ± 0.2	-0.05 ± 0.10					
			4	0.47 ± 0.01							
			6	0.75 ± 0.04							
			8	1.15 ± 0.02							
			10	1.51 ± 0.06							
100			2	0.26 ± 0.03	1.2 ± 0.1	-0.06 ± 0.08					
			4	0.39 ± 0.01							
			6	0.58 ± 0.02							
			8	0.96 ± 0.02							
			10	1.21 ± 0.06							
$\Delta H^\ddagger, \text{kJ mol}^{-1}$					$+78.9 \pm 1.4$						
$\Delta S^\ddagger, \text{J K}^{-1} \text{mol}^{-1}$					$+88 \pm 5$						
$\Delta V^\ddagger, \text{cm}^3 \text{mol}^{-1}$					$+23.1 \pm 1.6$						
$(\text{en})_2$	20.0	0.1	4	0.49 ± 0.06	1.16 ± 0.10	0.07 ± 0.07					
			6	0.75 ± 0.07							
			8	1.02 ± 0.04							
			10	1.22 ± 0.08							
			10	1.22 ± 0.08							
	25.0			2	0.62 ± 0.01	3.09 ± 0.08	0.05 ± 0.05				
				4	1.34 ± 0.08						
				5	1.62 ± 0.01						
				6	1.93 ± 0.07						
				8	2.46 ± 0.11						
	30.0			10	3.16 ± 0.10	4.03 ± 0.37	0.31 ± 0.26				
				4	1.82 ± 0.05						
				5	2.22 ± 0.12						
				6	2.99 ± 0.04						
				8	3.55 ± 0.15						
	35.0			10	4.25 ± 0.02	7.56 ± 0.62	0.10 ± 0.40				
				2	1.81 ± 0.02						
				4	3.11 ± 0.14						
				6	4.09 ± 0.08						
				8	6.49 ± 0.06						
24.3			10	7.68 ± 0.29							
			6	1.01 ± 0.04							
			5	0.81 ± 0.04							
			25	0.62 ± 0.05							
			50	0.62 ± 0.05							
			75	0.45 ± 0.02							
			100	0.32 ± 0.02							
			100	0.32 ± 0.02							
			$\Delta H^\ddagger, \text{kJ mol}^{-1}$					$+83 \pm 12$			
			$\Delta S^\ddagger, \text{J K}^{-1} \text{mol}^{-1}$					$+100 \pm 41$			
$\Delta V^\ddagger, \text{cm}^3 \text{mol}^{-1}$					$+27.8 \pm 0.9$						

^a[Fe(II)] = 4×10^{-5} M; ionic strength = 0.1 M (NaClO₄). ^bMean value of four to six kinetic runs.

Table II. k_{obs} as a Function of [Co(III)], Temperature, Pressure, and Light Intensity for the Reaction^a

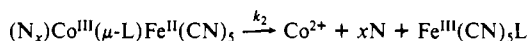
N_x	L	temp, °C	pressure, MPa	slit width, mm ^b	$10^4[\text{Co(III)}], \text{M}$	$k_{\text{obs}}, \text{s}^{-1}$ ^c	$\overline{k_{\text{obs}}}, \text{s}^{-1}$ ^d	
(NH ₃) ₄	pzc	19.9	0.1	1	2	(1.35 ± 0.01) × 10 ⁻²	(1.35 ± 0.01) × 10 ⁻²	
					4	(1.37 ± 0.02) × 10 ⁻²		
					5	(1.35 ± 0.01) × 10 ⁻²		
					8	(1.34 ± 0.02) × 10 ⁻²		
		25.0	1	10	1	4	(2.44 ± 0.03) × 10 ⁻²	(2.38 ± 0.09) × 10 ⁻²
						6	(2.44 ± 0.03) × 10 ⁻²	
						8	(2.41 ± 0.01) × 10 ⁻²	
						10	(2.33 ± 0.01) × 10 ⁻²	
		30.0	1	30	2	4	(5.14 ± 0.06) × 10 ⁻²	(5.15 ± 0.06) × 10 ⁻²
						6	(5.08 ± 0.08) × 10 ⁻²	
						8	(5.22 ± 0.07) × 10 ⁻²	
						10	(5.17 ± 0.05) × 10 ⁻²	
		35.0	1	10	1	4	(4.26 ± 0.09) × 10 ⁻²	(4.12 ± 0.10) × 10 ⁻²
						5	(3.97 ± 0.03) × 10 ⁻²	
						6	(4.14 ± 0.02) × 10 ⁻²	
						8	(4.10 ± 0.03) × 10 ⁻²	
		24.3	1	35.0	1	6	(4.12 ± 0.01) × 10 ⁻²	(7.55 ± 0.46) × 10 ⁻²
						8	(7.88 ± 0.02) × 10 ⁻²	
						8	(7.23 ± 0.02) × 10 ⁻²	
						10	(4.12 ± 0.01) × 10 ⁻²	
24.3	0.1			5	0.1	6	(1.38 ± 0.02) × 10 ⁻²	(7.55 ± 0.46) × 10 ⁻²
						25	(1.11 ± 0.01) × 10 ⁻²	
						50	(0.80 ± 0.02) × 10 ⁻²	
						75	(0.65 ± 0.03) × 10 ⁻²	
24.3	2	5	2	6	(0.48 ± 0.01) × 10 ⁻²	(7.55 ± 0.46) × 10 ⁻²		
				25	(5.3 ± 0.2) × 10 ⁻²			
				50	(4.5 ± 0.1) × 10 ⁻²			
				75	(4.6 ± 0.1) × 10 ⁻²			
24.3	2	100	2	6	(4.4 ± 0.3) × 10 ⁻²	(7.55 ± 0.46) × 10 ⁻²		
				25	(4.6 ± 0.1) × 10 ⁻²			
				50	(4.4 ± 0.3) × 10 ⁻²			
				100	(4.6 ± 0.1) × 10 ⁻²			
$\Delta H^\ddagger, \text{kJ mol}^{-1}$				1			83 ± 2	
$\Delta S^\ddagger, \text{J K}^{-1} \text{mol}^{-1}$				1			+2 ± 7	
$\Delta V^\ddagger, \text{cm}^3 \text{mol}^{-1}$				0.1		+27.3 ± 0.9		
				2		+3.0 ± 2.1		
(en) ₂ ^e	pzc	44.7	0.1	1	1	(12.7 ± 0.4) × 10 ⁻⁴		
					5	(10.3 ± 0.1) × 10 ⁻⁴		
					27	(7.7 ± 0.3) × 10 ⁻⁴		
					51	(6.1 ± 0.4) × 10 ⁻⁴		
					75	(4.8 ± 0.2) × 10 ⁻⁴		
					100	(3.4 ± 0.4) × 10 ⁻⁴		
$\Delta V^\ddagger, \text{cm}^3 \text{mol}^{-1}$						+28.4 ± 2.0		
(NH ₃) ₅	pz	24.2	5	0.1	10	(4.41 ± 0.01) × 10 ⁻²		
					25	(3.31 ± 0.02) × 10 ⁻²		
					50	(2.39 ± 0.02) × 10 ⁻²		
					75	(1.55 ± 0.05) × 10 ⁻²		
		24.2	2	100	0.1	10	(1.20 ± 0.10) × 10 ⁻²	
						5	(12.5 ± 0.4) × 10 ⁻²	
						25	(11.2 ± 0.1) × 10 ⁻²	
						50	(10.0 ± 0.2) × 10 ⁻²	
24.2	2	100	0.1	10	(8.88 ± 0.20) × 10 ⁻²			
				5	(8.88 ± 0.20) × 10 ⁻²			
				25	(8.88 ± 0.20) × 10 ⁻²			
				75	(8.34 ± 0.26) × 10 ⁻²			
$\Delta V^\ddagger, \text{cm}^3 \text{mol}^{-1}$				0.1		+34.6 ± 1.4		
				2		+10.6 ± 0.7		

^a [Fe(II)] = 4 × 10⁻⁵ M; ionic strength = 0.1 M (NaClO₄). ^b Slit width of Zeiss PMQ II monochromator. ^c Mean value of three to five kinetic runs. ^d Mean value of k_{obs} . ^e [Fe(II)] = 1 × 10⁻⁴ M.

reaction followed by a slower electron-transfer process. In many systems, the complex formation step is too fast to be measured. However, in the selected systems, the formation of the bridged intermediate can be followed by using stopped-flow techniques. In this way the rate constants for the formation and decomposition of the bridged intermediate (k_1 and k_{-1} , respectively) can be separated from the electron-transfer rate constant k_2 . Accordingly, the activation parameters for all steps can be separated and their sensitivity toward light can be studied.

Formation of a Bridged Intermediate. The formation of the bridged complex intermediates involves substitution of the solvent

molecule on Fe^{II}(CN)₅H₂O³⁻ by the available coordination site on L, and can be studied by using stopped-flow techniques. Kinetic measurements were performed under pseudo-first-order conditions by using an excess of the Co(III) complex. Preliminary experiments indicated that the corresponding observed rate constant was independent of the selected Fe(II) concentration and depended linearly on the Co(III) concentration. No significant effect of pH on the observed rate constant in the range 5 < pH < 9 could be detected. In addition, the intensity of the analyzing light at the wavelength selected to monitor the formation reaction had no measurable effect on the observed rate constants in all cases.

Table III. Rate and Activation Parameters for the Reaction

N_x	L	slit width	k_2 at 25 °C, s ⁻¹	ΔH^\ddagger , kJ mol ⁻¹	ΔS^\ddagger , J K ⁻¹ mol ⁻¹	ΔV^\ddagger , cm ³ mol ⁻¹	ref	
(NH ₃) ₄	pzc	1 mm	$(2.4 \pm 0.1) \times 10^{-2}$	83 ± 2	+2 ± 7		a	
		0.1 mm	$(1.38 \pm 0.02) \times 10^{-2}$					+27.3 ± 0.9
		2 mm	$(5.3 \pm 0.2) \times 10^{-2}$					
(en) ₂	pzc	1 mm	$(1.3 \pm 0.1) \times 10^{-2}$	95 ± 4	+40 ± 13	+3.0 ± 2.1	a	
			$(12.7 \pm 0.4) \times 10^{-4b}$					+28.4 ± 2.0
			<10 ⁻⁵					
(NH ₃) ₅	pz	0.1 mm	10.4×10^{-5}	103 ± 6	+75 ± 21	+24	a	
			$(4.41 \pm 0.01) \times 10^{-2}$					+34.6 ± 1.4
		2 mm	$(12.5 \pm 0.4) \times 10^{-2}$	130 ± 5	+165 ± 5	+10.6 ± 0.7	a	
		1.4 nm	$(5.5 \pm 0.5) \times 10^{-2}$					+37 ± 1
		$(4.6 \pm 0.1) \times 10^{-2}$				15		

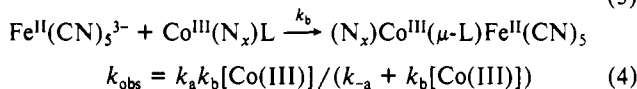
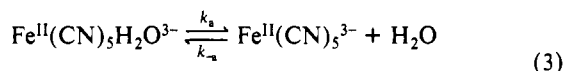
^aThis study; data from Table II. ^bTemperature = 45 °C.

The kinetic data as a function of [Co(III)], temperature and pressure, along with the calculated activation parameters, are summarized in Table I.

The kinetic data for the formation of the bridged species can be expressed in terms of the rate equation in (2). Plots of k_{obs}

$$k_{obs} = k_1[Co(III)] + k_{-1} \quad (2)$$

versus [Co(III)] are in general linear within the error limits of the data and exhibit meaningful intercepts (k_{-1}) only in the case of the tetraammine complex. In this case the pressure dependence of the reaction was studied for various [Co(III)], and k_1 and k_{-1} were determined at each pressure by combining the data from the different sets of experiments. This procedure resulted in fairly accurate k_1 but rather inaccurate k_{-1} values (see Table I). The values of k_1 , ΔH^\ddagger and ΔS^\ddagger are in close agreement with those reported before for both complexes.¹⁵ The activation parameters demonstrate that k_1 is characterized by large positive values for both ΔS^\ddagger and ΔV^\ddagger . This can be due to either a significant decrease in electrostriction due to charge neutralization during the formation of the bridged complex or the operation of a dissociative mechanism. In the latter case the forward reaction can be visualized as shown in (3), for which the rate law is given in (4).



$$k_{obs} = k_a k_b [Co(III)] / k_{-a} \quad (5)$$

Under the conditions of a linear dependence of k_{obs} on [Co(III)], (4) simplifies to (5), from which it follows that $k_1 = k_a k_b / k_{-a}$ when (5) is compared to (2). Both ΔS^\ddagger and ΔV^\ddagger are composite functions of the form given in (6). $\Delta V^\ddagger(k_{-a})$ is expected to be significantly

$$\Delta V^\ddagger = \Delta V^\ddagger(k_a) + \Delta V^\ddagger(k_b) - \Delta V^\ddagger(k_{-a}) \quad (6)$$

more negative than $\Delta V^\ddagger(k_b)$ since it involves bond formation with no change in electrostriction. Thus $\Delta V^\ddagger(k_b) - \Delta V^\ddagger(k_a)$ will result in an overall positive contribution toward ΔV^\ddagger . Similarly, $\Delta V^\ddagger(k_a)$ is also expected to be positive with a maximum value of ca. +13 cm³ mol⁻¹ estimated for the dissociation of a water molecule from an octahedral complex.²³ An experimental value of +13.5 ± 1.5 cm³ mol⁻¹ was reported²⁴ for the substitution reaction $Fe(CN)_5H_2O^{3-} + CN^- \rightarrow Fe(CN)_6^{4-} + H_2O$, which presumably involves the dissociation of a water molecule. It follows that the mechanism in (3) can quantitatively account for the large positive volumes an entropies of activation.

Electron-Transfer Process. The investigated electron-transfer reactions exhibit no significant dependence on pH in the range 5–9 but, in two of the three investigated complexes, a significant

dependence on the intensity of the analyzing beam. The reactions exhibit excellent first-order behavior under all experimental conditions, even where the photoinduced reaction markedly exceeded the thermal process. Preliminary experiments demonstrated that under pseudo-first-order conditions, i.e. excess of Co(III), the observed rate constant was independent of the Fe(II) concentration. The kinetic data are summarized in Table II, from which it follows that k_{obs} is independent of the employed [Co(III)]. The values of k_{obs} for the electron-transfer step are such that the formation of the bridged intermediate, as expressed by the rate equation in (2), is always complete and does not interfere with this reaction step (compare the data in Tables I and II) under all conditions. In addition, the kinetic data for the $Co(NH_3)_4(pzc)^{2+}$ and $Co(NH_3)_5pz^{3+}$ complexes exhibit a meaningful dependence on the slit width of the monochromator, i.e. the intensity of the analyzing light, whereas no significant dependence was found for the $Co(en)_2(pzc)^{2+}$ complex. These observations and the values of k_{obs} , ΔH^\ddagger and ΔS^\ddagger in Table II are in good agreement with those reported before.^{13–15} An overall comparison of the available rate and activation parameters for the electron-transfer process is given in Table III.

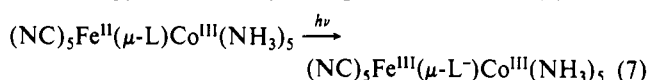
The activation volumes for the thermal electron-transfer reactions are all large and positive and in good agreement with those reported for two of the systems in the literature.^{13,14} Furthermore, these values are very close to those found for the outer-sphere electron-transfer reaction between various $Co(NH_3)_4(NH_2R)X^{(3-n)+}$ complexes (R = H, CH₃, and *i*-C₄H₉; Xⁿ⁻ = H₂O, py, DMSO, N₃⁻ and Cl⁻) and $Fe(CN)_6^{4-}$, for which ΔV^\ddagger varies between +19 and +34 cm³ mol⁻¹.^{25–27} The similarity in the ΔV^\ddagger values encourages us to interpret the present findings along the same line of argument. During the electron-transfer step, the Co(III) complex is reduced to Co(II) and Fe(II) is oxidized to Fe(III). The reduction process is expected to be accompanied by an intrinsic volume increase of ca. 20 cm³ mol⁻¹, whereas the oxidation step should result in an volume increase of ca. 40 cm³ mol⁻¹ mainly due to the decrease in electrostriction on going from $Fe^{II}(CN)_5^{3-}$ to $Fe^{III}(CN)_5^{2-}$ (compare the even larger difference for $Fe(CN)_6^{4-}$ and $Fe(CN)_6^{3-}$).^{13,25} Thus electron transfer may cause an overall volume increase as large as 60 cm³ mol⁻¹. This means that on a volume basis the transition state for the electron-transfer process lies approximately halfway between the reactant and product states. Before the electron transfer actually occurs (since no molecular dimensions change during the electron-transfer step itself), the bridged molecule rearranges to such an extent that Co(III) partially assumes a Co(II) character and Fe(II) partially assumes an Fe(III) character. Thus the energetics of the system reaches a point at which the electron can either be associated with the Fe center or with the Co center without involving significant energy barriers. This is according to our understanding the situation in the transition state, and electron

(23) Swaddle, T. W. *Inorg. Chem.* **1983**, *22*, 2663.(24) Finston, M. I.; Drickamer, H. G. *J. Phys. Chem.* **1981**, *85*, 50.(25) Krack, I.; van Eldik, R. *Inorg. Chem.* **1986**, *25*, 1743.(26) Krack, I.; van Eldik, R. *Inorg. Chem.* **1989**, *28*, 851.(27) Krack, I.; van Eldik, R. *Inorg. Chem.* **1990**, *29*, 1700.

transfer then occurs to produce the reaction products. In this way we account for the almost 50% overall volume change in terms of ΔV^\ddagger . An important aspect of our suggestion is that the large positive ΔV^\ddagger mainly results from volume changes associated with the iron center in agreement with arguments presented before.^{14,25,27}

We now turn to a discussion of the light-induced electron-transfer reaction. The significant increase in k_2 with increasing light intensity found in this study is in good agreement with similar findings reported before.^{13,15} The bridged complexes exhibit MLCT bands around 625 nm such that irradiation at this wavelength (usually selected to monitor the thermal redox reaction) results in a photoinduced electron-transfer process. The quantum yield for the latter process was reported¹⁵ to be 0.9 ± 0.15 for $\text{Co}(\text{NH}_3)_4(\text{pzc})^{2+}$ and $\text{Co}(\text{NH}_3)_5(\text{pz})^{3+}$ and 0.020 for $\text{Co}(\text{en})_2(\text{pzc})^{2+}$, which accounts for the fact that no significant effect of light intensity was observed in the latter case. A very significant finding of this study is that, under the conditions where a significant acceleration by light occurs, the observed pressure dependence almost completely disappears. For the $\text{Co}(\text{NH}_3)_4(\text{pzc})^{2+}$ complex the rate constant increases by almost a factor 4 such that the thermal reaction makes only a small contribution at high light intensities. In the case of the $\text{Co}(\text{NH}_3)_5(\text{pz})^{3+}$ complex, some contribution from the thermal reaction is still possible at high light intensities, and in fact a correction for this contribution results in an almost zero volume of activation for the photoinduced process.

The pressure independence of the photoinduced electron-transfer process can be interpreted in the following way. During MLCT excitation electron density is transferred from Fe(II) to the pyrazine or pyrazinecarboxylate ligand as shown in (7).¹⁵ The



subsequent first-order process observed during irradiation must involve the transfer of the electron from the bridging ligand to the cobalt center. According to the pressure independence of this process, no significant volume change is associated with this reaction, which means that the major volume increase occurs during

the oxidation of Fe(II). Our observation that the subsequent reduction of Co(III) following MLCT excitation does not lead to a significant volume increase directly supports our earlier arguments (see above) presented to account for the ΔV^\ddagger data associated with the thermally induced electron-transfer reaction.^{14,25–27} In general, this finding does contradict earlier arguments in favor of the suggestion that the major volume change that occurs in related electron-transfer reactions is associated with volume changes on the cobalt center.^{13,28} It must be kept in mind that the quantum yield for these photoinduced reactions is almost unity. This means that other deactivation routes than the photochemical reaction (i.e. radiationless and radiative deactivation) play no significant role. This would require that the lifetime of the MLCT excited state must be long so that electron transfer from the coordinated N atom to the Co(III) center can occur. Since the quantum yield is close to unity, any effect of pressure on the photochemical rate constant will not affect the quantum yield. This means that $\text{Fe}^{\text{III}}(\mu\text{-L}^-)\text{Co}^{\text{III}}$ is produced rapidly during the continuous irradiation and undergoes L-to-Co(III) electron transfer during the first-order decay.

We believe that the results of this investigation support the operation of a two-step electron-transfer mechanism for the photoinduced intramolecular redox process, i.e. the chemical mechanism.²⁹

Acknowledgment. We gratefully acknowledge financial support from the Deutsche Forschungsgemeinschaft, Fonds der Chemischen Industrie, and Volkswagen-Stiftung. A stipend from the Junta de Andalucia, which enabled P.G. to participate in this study, is greatly appreciated. Stimulating discussions with Dr. J. Burgess (University of Leicester, Leicester, U.K.) on the investigated reactions are kindly acknowledged.

Registry No. $\text{Fe}(\text{CN})_5\text{H}_2\text{O}^{3-}$, 18497-51-3; $\text{Co}(\text{NH}_3)_4\text{pzc}^{2+}$, 61546-76-7; $\text{Co}(\text{en})_2\text{pzc}^{2+}$, 56238-31-4; $(\text{NH}_3)_4\text{Co}^{\text{III}}(\mu\text{-pzc})\text{Fe}^{\text{II}}(\text{CN})_5$, 61546-71-2; $(\text{en})_2\text{Co}^{\text{III}}(\mu\text{-pzc})\text{Fe}^{\text{II}}(\text{CN})_5$, 56238-33-6; $(\text{NH}_3)_5\text{Co}^{\text{III}}(\mu\text{-pz})\text{Fe}^{\text{II}}(\text{CN})_5$, 66840-84-4.

(28) Kanesato, M.; Ebihara, M.; Sasaki, Y.; Saito, K. *J. Am. Chem. Soc.* **1983**, *105*, 5711.

(29) Gould, E. S. *Acc. Chem. Res.* **1985**, *18*, 22.

Contribution from the Department of Chemistry and the Center for Organometallic Research, University of North Texas, Denton, Texas 76203-5068, and Institute for Inorganic Chemistry, University of Witten/Herdecke, Stockumer Strasse 10, 5810 Witten, FRG

Octahedral Metal Carbonyls. 71.¹ Kinetics and Mechanism of Benzene Displacement from Photogenerated $[(\eta^2\text{-Benzene})\text{Cr}(\text{CO})_5]$

Shulin Zhang,² Gerard R. Dobson,*² Volker Zang,³ Hari C. Bajaj,³ and Rudi van Eldik*³

Received December 7, 1989

Pulsed laser flash photolysis of $\text{Cr}(\text{CO})_6$ in $\text{Cr}(\text{CO})_6/\text{benzene}/\text{L}$ solutions (L = piperidine, 1-hexene, pyridine) affords as the predominant reaction species $[(\eta^2\text{-benzene})\text{Cr}(\text{CO})_5]$ (**1**) in which benzene is coordinated to Cr via an "isolated" C=C bond. **1** reacts with L on the microsecond time scale to afford $\text{LCr}(\text{CO})_5$ products. On the basis of kinetics studies over a wide range of benzene and L concentrations ($[\text{benzene}] = 2.8\text{--}10.1\text{ M}$; $[\text{L}] = 1.2\text{--}6.5\text{ M}$), a temperature range of 5–35 °C, pressures to 100 MPa, and isotopic labeling studies (benzene-*d*₆), it is concluded for L = 1-hexene and piperidine that the displacement of benzene from **1** takes place by means of reversible formation of the $[\text{Cr}(\text{CO})_5]$ intermediate via a transition state in which benzene is bonded to Cr, forming a "σ-complex", or via an agostic C–H–Cr interaction. For L = pyridine at very high [py], an interchange process involving displacement of benzene also may be accessible. The observed rate laws incorporate the concentrations of all chemical species present in solution in significant concentration after flash photolysis. Thus benzene/L solutions may be classified as "reactive solutions" in the presence of $[\text{Cr}(\text{CO})_5]$. The upper limit of the benzene–Cr bond strength is estimated from activation data to be 9.4 (1) kcal/mol.

Introduction

Coordinationally unsaturated transition-metal complexes are of increasing interest because they often are implicated as active

species in homogeneous catalysis. In this regard it has been noted that "a site of coordinative unsaturation is perhaps the single important property of a homogeneous catalyst".⁴ However, it is now widely recognized that in many cases the species produced in predominant concentration after metal–ligand bond fission are

(1) Part 70: Zhang, S.; Dobson, G. R. *Inorg. Chim. Acta* **1989**, *165*, 11.

(2) University of North Texas.

(3) University of Witten/Herdecke.

(4) Collman, J. P. *Acc. Chem. Res.* **1968**, *1*, 136.